Published in final edited form as:
Neuron. 2012 June 7; 74(5): . doi:10.1016/j.neuron.2012.03.039.

Mg^{2+} Block of *Drosophila*

Tomoyuki Miyashita[1], **Yoshiaki Oda**[2], **Junjiro Horiuchi**[3], **Jerry C.P. Yin**[4], **Takako Morimoto**[2], and **Minoru Saitoe**[1,*]

[1]Tokyo Metropolitan Institute of Medical Science, Setagaya, Tokyo 156-8502, Japan

[2]Laboratory of Cellular Neurobiology, School of Science, Tokyo University of Pharmacy and Lifesciences, Hachioji, Tokyo 192-0392, Japan

[3]Center for Priority Areas, Tokyo Metropolitan University, Hachioji, Tokyo 192-0397, Japan

[4]Departments of Genetics and Psychiatry, University of Wisconsin at Madison, Madison, WI 53706-3434, USA

SUMMARY

NMDA receptor (NMDAR) channels allow Ca^{2+} influx only during correlated activation of both pre- and postsynaptic cells; a Mg^{2+} block mechanism suppresses NMDAR activity when the postsynaptic cell is inactive. Although the importance of NMDARs in associative learning and long-term memory (LTM) formation has been demonstrated, the role of Mg^{2+} block in these processes remains unclear. Using transgenic flies expressing NMDARs defective for Mg^{2+} block, we found that Mg^{2+} block mutants are defective for LTM formation but not associative learning. We demonstrate that LTM-dependent increases in expression of synaptic genes, including *homer*, *staufen*, and *activin*, are abolished in flies expressing Mg^{2+} block defective NMDARs. Furthermore, we show that genetic and pharmacological reduction of Mg^{2+} block significantly increases expression of a CREB repressor isoform. Our results suggest that Mg^{2+} block of NMDARs functions to suppress basal expression of a CREB repressor, thus permitting CREB-dependent gene expression upon LTM induction.

INTRODUCTION

Ca^{2+} enters a cell through NMDAR channels only when presynaptic glutamate release and depolarization of the postsynaptic membrane occur simultaneously (correlated activity). Conversely, NMDAR-mediated Ca^{2+} influx is suppressed at voltages near the resting membrane potential (uncorrelated activity), due to Mg^{2+} block, a mechanism in which the pore of NMDARs is blocked by external Mg^{2+} ions (Mayer et al., 1984; Nowak et al., 1984). Since Mg^{2+} block allows cells to discriminate between correlated synaptic inputs and uncorrelated activity, NMDARs have been proposed to function as “Hebbian coincidence detectors.” However, the behavioral significance and molecular effects of Mg^{2+}-block-dependent suppression of Ca^{2+} influx during uncorrelated activity remains unknown (Single et al., 2000).

Functional NMDARs are heteromeric assemblies of an essential NR1 subunit and various NR2 subunits. Studies of NMDAR channels have demonstrated that Mg^{2+} block is

*Correspondence: saito-mn@igakuken.or.jp.

SUPPLEMENTAL INFORMATION

Supplemental Information includes one table, eight figures, and Supplemental Experimental Procedures and can be found with this article online at doi:10.1016/j.neuron.2012.03.039.

dependent on an asparagine (N) residue at a "Mg^{2+} block site" located in a putative channel-forming transmembrane segment (TM2, see Figure 2A) of each subunit (Burnashev et al., 1992; Mori et al., 1992; Single et al., 2000). *Drosophila* have a single NR2 homolog, dNR2, which contains a glutamine at the Mg^{2+} block site (Q721), and a single NR1 homolog, dNR1, which contains an N at this site (N631). A previous study has shown that the N631 residue in dNR1 is sufficient for Mg^{2+} block in flies (Xia et al., 2005).

In *Drosophila*, early labile memory formed after Pavlovian olfactory associative learning is consolidated into two longer lasting memory phases: long-term memory (LTM), which requires new gene expression and protein synthesis, and anesthesia-resistant memory (ARM), which can be formed in the presence of transcriptional and translational inhibitors (Tully et al., 1994). In both vertebrates and invertebrates, a transcription factor, CREB, plays a critical role in gene expression required for LTM formation (Bourtchuladze et al., 1994; Yin et al., 1994). While previous studies have shown that hypomorphic mutations in *Drosophila* NMDARs (dNMDARs) disrupt both associative learning (LRN) and LTM formation without affecting ARM (Wu et al., 2007; Xia et al., 2005), it is still not clear how Mg^{2+} block is involved in these processes.

To understand the functional significance of Mg^{2+} block in dNMDARs, we generated transgenic flies expressing *dNR1* mutated at the Mg^{2+} block site, *dNR1*(*N631Q*), in neurons. Strikingly, we found that these Mg^{2+} block mutant flies are defective for LTM formation but not LRN. We show that Mg^{2+} block functions to suppress basal expression of a repressor isoform of *Drosophila* CREB during uncorrelated activity. This allows increased CREB-dependent gene expression to occur during correlated activity, leading to formation of LTM.

RESULTS

Reduced Mg^{2+} Block in Transgenic Flies Expressing *dNR1*(*N631Q*)

Immunohistochemical studies using antibodies to dNR1 demonstrate that dNMDARs are expressed throughout the *Drosophila* brain (Figure S1 available online) (Xia et al., 2005; Zachepilo et al., 2008; Zannat et al., 2006). Therefore, we used an *elav-GAL4/UAS-GFP* (*elav/GFP*) transgenic line (Brand and Perrimon, 1993), which expresses GFP in neurons, to characterize endogenous dNMDARs in pupal primary cultured neurons (Figure 1A). Using whole-cell patch clamp, we determined that more than 85% of GFP-positive cells showed NMDA-induced inward currents at a −80mV membrane potential in the absence of external Mg^{2+} (119 out of 136 cells, Figure 1B). These responses were blocked by physiological concentrations of 20 mM Mg^{2+} (Stewart et al., 1994). In addition, mammalian NMDAR antagonists, APV and MK801, significantly suppressed NMDA-activated currents (Figure 1C). These results demonstrate that endogenous dNMDARs are widely expressed in neurons of the fly brain and have similar physiological and pharmacological properties to mammalian NMDARs.

We overexpressed either wild-type *dNR1*(*wt*) or Mg^{2+}-block-site-mutated *dNR1*(*N631Q*) transgenes (Figure 2A) in neurons using an *elav-GAL4* driver*: elav-GAL4*/*UAS-dNR1*(*wt*), [*elav/dNR1*(*wt*)], and *elav-GAL4/UAS-dNR1*(*N631Q*), [*elav/dNR1*(*N631Q*)]. Overexpression of dNR1(wt) and dNR1(N631Q) proteins was confirmed by western blots (Figure S2). As seen in Figure 2B, all dNMDAR-mediated currents in neurons from *elav/dNR1*(*wt*) pupae showed significant Mg^{2+} block in the presence of Mg^{2+}, a result similar to what was seen in neurons from wild-type pupae. In contrast, Mg^{2+} block of dNMDAR-mediated currents was abolished in neurons from *elav/dNR1*(*N631Q*) pupae. I-V curves of *elav/dNR1*(*N631Q*) pupae in the presence or absence of Mg^{2+} were identical at membrane potentials of −80 mV or above, indicating that overexpression of *dNR1*(*N631Q*) dominantly suppresses Mg^{2+} block.

Notably, the *dNR1*(*N631Q*) mutation does not alter the dose-dependent responsiveness to NMDA in the absence of Mg^{2+} (Figure S3A). Furthermore, in contrast to *elav/dNR1*(*wt*) cells, NMDA-induced currents remain constant at different Mg^{2+} concentrations in *elav/dNR1*(*N631Q*) cells (Figure S3B), suggesting that the N631Q mutation alters Mg^{2+} sensitivity without altering channel pharmacology.

LTM Is Disrupted in *elav/dNR1*(*N631Q*) Flies

Hypomorphic mutations in *dNR1* (*dNR1*^{EP3511} and *dNR1*^{EP331}) disrupt learning (LRN), memory measured immediately after aversive olfactory conditioning, and short-term memory (STM), assayed 1 hr after training (Figures 3A and 3B) (Xia et al., 2005). In contrast, both LRN and STM are normal in *elav/dNR1*(*N631Q*) flies, as well as in transgenic control *elav/dNR1*(*wt*) flies (Figures 3A and 3B).

To investigate the role of Mg^{2+} block in associative learning in more detail, we measured LRN after short-duration training, a modified short-program training protocol for which learning is plotted as a function of training duration (Cheng et al., 2001). As seen in Figure 4A, as training duration increases, LRN scores increase up to a maximum plateau. While this increase is inhibited in hypomorphic *dNR1*^{EP3511} and *dNR1*^{EP331} mutants, it is slightly enhanced in *elav/dNR1*(*N631Q*) flies. Strikingly, the LRN defects in hypomorphic *dNR1* mutants is rescued by expressing *dNR1*(*N631Q*) in neurons (Figure 4B), suggesting Mg^{2+} block may not be required for learning.

Mg^{2+} block has been proposed to restrict dNMDAR activation to cells receiving coincident stimulation. Thus, lack of Mg^{2+} block may activate dNMDARs in more neurons than is normal during olfactory conditioning, creating a situation in which the conditioned response may not be restricted to the conditioned odor. To test this possibility, we performed olfactory conditioning by pairing a single CS+ odor with electric shocks and then test measured escape responses to the CS+ odor as well as unrelated odors. As seen in Figure S4, when *elav/dNR1*(*N631Q*) flies are conditioned to OCT, avoidance of OCT increases compared to nonconditioned controls, while avoidance of MCH and benzaldehyde (BA) does not, suggesting that odor specificity during learning remains intact in *elav/dNR1*(*N631Q*) flies.

Besides causing defects in learning, hypomorphic mutations in dNR1 also cause significant reductions in LTM (Figure 3C) (Xia et al., 2005), assayed as one-day memory after spaced training (ten training sessions with rest intervals between each training), while it has no effect on ARM (Figure 3D), one-day memory after massed training (ten training sessions without rest intervals). Similar to hypomorphic mutants, *elav/dNR1* (*N631Q*) flies displayed a significant decrease in one-day memory after spaced training (Figure 3C) but not after massed training (Figure 3D). We also observed similar defects in LTM formation in a second independent *elav/dNR1*(*N631Q*) line (Figure S5). As expected from their normal learning scores, *elav/dNR1*(*N631Q*) flies exhibit normal responses when tested for odor acuity and shock reactivity (data not shown), suggesting that Mg^{2+} block of dNMDARs is required specifically for LTM formation.

Since NMDAR activity is required for formation of neural networks (Adesnik et al., 2008; Bellinger et al., 2002; Hirasawa et al., 2003; Lüthi et al., 2001; Tian et al., 2007), LTM defects in *elav/dNR1*(*N631Q*) flies may arise from abnormal development of networks required for LTM. To determine whether Mg^{2+} block is required acutely during LTM formation or whether it is required during development, we expressed the *dNR1*(*N631Q*) transgene using an *elav-GeneSwitch* driver (*elav-GS*), which expresses the transgene in neurons only when flies are fed RU486 (Mao et al., 2004; Osterwalder et al., 2001). Feeding 1 mM RU486 one day before training significantly disrupted LTM (Figure 4C) but not

ARM formation (data not shown) in *elav-GS/dNR1*(*N631Q*) flies, while it had no effect on *elav-GS/dNR1*(*wt*) flies. LTM was normal in both lines in the absence of RU486. Thus, Mg^{2+} block is likely to be required during LTM formation/recall and may not be required during development of LTM circuits.

Previous results (Wu et al., 2007) demonstrate that NMDARs are required in the central complex for LTM formation. Consistent with this finding, we found that expression of *dNR1*(*N631Q*) in the ellipsoid body of the central complex abolishes LTM (Figure 4D) but not ARM (data not shown). Furthermore, we found that expressing *dNR1*(*N631Q*) in the mushroom bodies (MBs) also has the same effect (Figure 4D and data not shown for ARM).

High Ca^{2+} permeability is required for NMDAR-mediated Ca^{2+} signaling and studies of mammalian NMDAR channels have demonstrated that an N/Q substitution at the Mg^{2+} block site in NR1 reduces Ca^{2+} permeability of NMDARs (Burnashev et al., 1992; Single et al., 2000). This raised the possibility that the LTM defect we observed in our *N631Q* mutants might be due to reduced Ca^{2+} influx rather than altered Mg^{2+} block. To address this issue, we compared reversal potentials in high Na^{+} extracellular solution ($V_{rev,Na}$) and in high Ca^{2+} extracellular solution ($V_{rev,Ca}$) between *elav/dNR1*(*wt*) and *elav/dNR1*(*N631Q*) flies (Chang et al., 1994; Single et al., 2000; Skeberdis et al., 2006). As seen in Figure 2C, we observed similar $V_{rev,Na}$ and $V_{rev,Ca}$ between genotypes ($p > 0.09$ for $V_{rev,Na}$; $p > 0.1$ for $V_{rev,Ca}$). Consequently, the relative Ca^{2+} permeability (P_{Ca}/P_{Na}) calculated using the Goldman-Hodgkin-Katz (GHK) equation was not significantly different in these two lines ($p > 0.09$). These results indicate that in contrast to mammalian NR1, the N/Q substitution at the Mg^{2+} block site of dNR1 does not attenuate Ca^{2+} permeability and suggests that the LTM defect observed in *elav/dNR1*(*N631Q*) flies is not due to decreased Ca^{2+} permeability.

Induction of LTM-Associated Genes Is Disrupted in *elav/dNR1*(*N631Q*) Flies

To determine what aspect of LTM formation is defective in *elavdNR1*(*N631Q*) flies, we first examined the expression of several genes associated with LTM and late-phase LTP (L-LTP), including *staufen*, *homer*, and *activin*, as well as other genes involved in synaptic plasticity, including *dlg* and *14-3-3ζ*. *staufen* expression has been shown to increase significantly after training that induces LTM (Dubnau et al., 2003), and *activin* and *homer* expression increase upon induction of L-LTP in an NMDAR-dependent manner (Inokuchi et al., 1996; Kato et al., 1997; Rosenblum et al., 2002). In contrast, PSD-95, the mammalian homolog of Dlg is required for normal synaptic plasticity (Ehrlich and Malinow, 2004), but its expression does not change during this process (Kuriu et al., 2006). The *Drosophila* 14-3-3ζ protein, *leonardo*, is involved in olfactory associative learning (Skoulakis and Davis, 1996), but changes in its expression due to training have not been described.

We observed significant increases in *activin*, *homer*, and *staufen* expression in spaced trained flies, compared to naive or massed trained flies (Figure 5). In comparison, we did not observe any differences in expression of *dlg* and *14-3-3ζ* between spaced trained and massed trained flies.

Hypomorphic *dNR1* (*dNR1*^{EP3511}) flies showed defects in LTM-dependent increases in *activin*, *homer*, and *staufen* expression (Figure 6A), indicating that these increases are NMDAR-dependent. Significantly, increased expression of *activin*, *homer*, and *staufen* was observed in *elav/dNR1*(*wt*) flies after training, while these increases were completely absent in *elav/dNR1* (*N631Q*) flies (Figure 6B). Since *dNR1*^{EP3511} flies have fewer dNMDARs, dNMDAR-mediated Ca^{2+} influx during spaced training is likely to be decreased, preventing increased *activin*, *homer*, and *staufen* expression. On the other hand, *elav/dNR1* (*N631Q*) flies should have normal Ca^{2+} influx during spaced training but increased Ca^{2+} influx during uncorrelated activity at the resting state. These results suggest that proper expression of

LTM-associated genes has two requirements: first, an increase in dNMDAR activity during spaced training must occur; and second, inappropriate dNMDAR activity at the resting state must be inhibited by Mg^{2+} block.

To further characterize LTM-dependent gene expression and the effect of Mg^{2+} block on this expression, we analyzed *homer* in more depth and determined that *Drosophila homer* mutants are normal for LRN and ARM but have specific defects in LTM (Figure S6). Expression of HOMER protein significantly increases in neuropil regions, including the protocerebral bridge (PB), calyces (Cas) of the MBs, lateral protocerebrum (LP), and antennal lobes (ALs) after spaced training in *elav/dNR1*(*wt*) flies. However, these increases are not observed in *elav/dNR1* (*N631Q*) flies (Figure 6C). In particular, when *dNR1*(*N631Q*) is expressed in the MBs, it suppresses increases in HOMER protein in the Cas but not in other regions, such as the PB (Figure 6C), suggesting a cell-autonomous requirement of Mg^{2+} block in LTM-dependent gene expression.

Transcriptional Activity of CREB Is Disrupted in *elav/dNR1*(*N631Q*) Flies

Why is Mg^{2+} block required for increases in *activin*, *homer*, and *staufen* expression upon LTM induction? The transcription factor CREB plays a critical role in LTM and L-LTP formation (Barco et al., 2002; Silva et al., 1998; Yin and Tully, 1996). In *Drosophila,* the balance between activator and repressor forms of CREB is important for transcriptional activity, and overexpression of the dCREB2-b repressor prior to spaced training prevents LTM formation without affecting other memory phases (Yin et al., 1994). Notably, the enhancer/promoter region of the gene encoding the βA subunit of activin contains a CRE site (Tanimoto et al., 1996), and *homer* expression is regulated by ERK, a member of the MAPK family, which activates CREB-dependent transcription (Kato et al., 2003; Rosenblum et al., 2002). These data suggest that training-dependent increases in *activin*, *homer*, and *staufen* may require CREB activity. Thus, we examined the expression of these genes in *hs-dCREB2-b* flies, which express the *dCREB2-b* repressor under heat-shock promoter control (Yin et al., 1994). In the absence of heat shock, *hs-dCREB2-b* flies showed significant increases in expression of all three genes after spaced training (data not shown). However, *hs-dCREB2-b* flies heat shocked for 30 min at 35°C, 3 hr prior to spaced training did not show these increases (Figure 7A), indicating that LTM-dependent expression of these genes requires CREB activity.

Since LTM-dependent expression of *homer*, *staufen*, and *activin* is abolished either by removal of Mg^{2+} block or by increasing dCREB2-b amounts, we suspected that Mg^{2+} block may be required to regulate basal dCREB2-b expression. To address this point, we looked at expression of the dCREB2-b repressor isoform in *elav/dRN1*(*N631Q*) fly head extracts. Strikingly, we found a greater than 4-fold increase in *dCREB2-b* repressor transcripts in *elav/dNR1*(*N631Q*) heads (Figure 7B). dCREB2-b protein was also similarly increased nearly 4-fold in *elav/dNR1*(*N631Q*) head protein extracts compared to wild-type, *elav/dNR1*(*wt*), and $dNR1^{EP3511}$ extracts (Figure 7C). While expression of total *dCREB2* (including both activator and repressor isoforms) is also increased in *elav/dNR1*(*N631Q*) flies, the *dCREB2-b* to $dCREB2_{total}$ ratio (*dCREB2-b*/$dCREB2_{total}$) is increased nearly 3-fold in *elav/dNR1*(*N631Q*) flies as compared to wild-type and *elav/dNR1*(*wt*) flies (Figure 7D). These results indicate that the increase in total *dCREB2* expression is predominantly due to an increase in *dCREB2-b* repressor expression and suggest that one function of Mg^{2+} block is to inhibit *dCREB2-b* expression, thus allowing dCREB2-dependent gene expression upon LTM induction.

To further test this possibility, we examined whether removal of external Mg^{2+} increases amounts of dCREB2-b in a wild-type background. We measured amounts of dCREB2-b protein in isolated single wild-type brains cultured in Mg^{2+}-free medium, which contained

100 μM TTX in order to block correlated activation of dNMDARs. After a 2 hr incubation, we observed significant increases in amounts of dCREB2-b compared to amounts in brains cultured in 20-mM-Mg^{2+} medium (Figure 7E). The increase in dCREB2-b in Mg^{2+}-free medium is strongly suppressed by the NMDAR antagonist MK801 and by dNR1 mutation, suggesting that in the absence of Mg^{2+} block, Ca^{2+} entry through dNMDARs increases dCREB2-b protein levels.

We next wanted to determine whether the increase in dCREB2-b expression observed in *elav/dNR1*(*N631Q*) flies is sufficient to inhibit LTM formation. Thus, we plotted one-day memory scores after spaced training as a function of dCREB2-b protein levels in wild-type and *hs-dCREB2-b* flies heat shocked for various durations. As seen in Figure 8A, defects in LTM formation were highly correlated with dCREB2-b protein expression. Heat-shocked wild-type flies and non-heat-shocked *hs-dCREB2-b* flies had normal one-day memory and similar dCREB2-b expression. On the other hand, *hs-dCREB2-b* flies expressed increasing amounts of dCREB2-b protein upon increasing heat-shock duration. This increase in dCREB repressor expression was correlated with a decrease in one-day memory in a linear fashion in the range tested. Significantly, we found that data from *elav/dNR1*(*wt*) and *elav/dNR1*(*N631Q*) flies plotted on the same graph fit the same regression line as our *hs-dCREB2-b* data; *elav/dNR1*(*wt*) flies expressed wild-type levels of dCREB2-b and had one-day memory scores comparable to wild-type and non-heat-shocked *dCREB2-b* flies, while *elav/dNR1*(*N631Q*) flies expressed similar amounts of dCREB2-b and had similar memory to *hs-dCREB-2b* flies heat shocked for 30 min. In contrast, $dNR1^{EP3511}$ flies did not show any increases in dCREB2-b mRNA or protein but had poor LTM scores (see also Figures 7B and 7C). These results indicate that the increase in expression of the dCREB2-b repressor in Mg^{2+} block mutants is correlated with and sufficient to cause the decrease in LTM observed in these mutants, while memory defects in *dNR1* hypomorphs likely occurs through a different mechanism.

DISCUSSION

Although the mechanism through which Mg^{2+} block restricts NMDAR activity is well known, the cellular and behavioral functions of Mg^{2+} block have not been extensively studied. In this study, we used transgenic flies expressing *dNR1*(*N631Q*) to show that Mg^{2+} block is important for formation of LTM.

Previous studies of hypomorphic mutants have shown that NMDARs are required for both learning and LTM. In contrast, our Mg^{2+} block mutants do not have learning defects. This suggests that although Ca^{2+} influx through NMDARs is important for learning, inhibition of influx during uncorrelated activity is not. Notably, *elav/dNR1*(*N631Q*) flies have slightly enhanced learning. Consistent with this result, NMDAR-dependent induction of hippocampal LTP is enhanced in the absence of external Mg^{2+} (Mizuno et al., 2001). In our studies, we have over-expressed Mg^{2+}-block-defective dNR1 in an otherwise wild-type background, so we cannot definitively conclude that Mg^{2+} block is dispensable for learning. However, electrophysiology experiments indicate that Mg^{2+} block is abolished in our flies at physiological potentials. Furthermore, we demonstrate that expression of Mg^{2+}-block-defective *dNR1* rescues learning defects in *dNR1* hypomorphs, consistent with a model in which Mg^{2+} block is not required for learning. Interestingly, our *dNR1*(*N631Q*) transgene does not rescue the semilethality of *dNR1* hypomorphs, suggesting that Mg^{2+} block has an essential biological function unrelated to learning.

Our results suggest that Mg^{2+}-block-dependent suppression of NMDAR activity and Ca^{2+} influx at the resting state is critical for LTM formation. Supporting this idea, chronic reduction of NMDAR-mediated Ca^{2+} influx at the resting state has been shown to enhance

long-term synaptic plasticity (Slutsky et al., 2004) and LTM (Slutsky et al., 2010). Extending these results, we found that Mg^{2+} block is required for CREB-dependent gene expression during LTM formation. A CREB-dependent increase in *staufen* expression upon spaced training is essential for LTM formation (Dubnau et al., 2003), and we show that Mg^{2+} block is required for this increase. We also identified two other genes, *activin* and *homer*, that are expressed upon LTM induction in a CREB-dependent manner. We propose that all three genes are maintained in an LTM-inducible state by Mg^{2+}-block-dependent inhibition of CREB repressor and show that the amount of increase in expression of dCREB2-b in Mg^{2+} block mutants correlates with the ability of dCREB2-b to suppress LTM. The 4-fold increase in dCREB2-b protein in Mg^{2+} block mutant flies is comparable to the increase in dCREB2-b in heat-shocked *hs-dCREB2-b* flies showing equivalent defects in LTM.

We next characterized the *homer* gene further and determined that it is required specifically for LTM but not for learning or ARM. We determined that spaced training increases HOMER expression in several brain regions, including the antennal lobes, lateral protocerebrum, protocerbral bridge, and calyx of the MBs. This increase does not occur in the absence of Mg^{2+} block. Significantly, when Mg^{2+} block is abolished by *dNR1*(*N631Q*) expression, specifically in the MBs, increased Homer expression is suppressed in the MBs but not in other regions, including the protocerebral bridge, indicating that Mg^{2+} block regulates CREB repressor and LTM-associated gene expressions in a cell autonomous manner.

Our electrophyisiological experiments demonstrate that 20 mM Mg^{2+} is sufficient to block *Drosophila* NMDAR currents at the resting potential (−80 mV). Although this concentration is higher than the concentrations needed to block mammalian NMDARs (Mayer et al., 1984; Nowak et al., 1984), the Mg^{2+} concentration in *Drosophila* hemolymph has been shown by various groups to be between 20 and 33 mM (Begg and Cruickshank, 1963; Croghan and Lockwood, 1960; Stewart et al., 1994), which is correspondingly higher than the Mg^{2+} concentration reported in mammalian plasma. In mammals, Mg^{2+} concentration is higher in cerebrospinal fluid than in plasma (McKee et al., 2005), further suggesting that the 20 mM Mg^{2+} concentration used in our study is likely to be within the physiologically relevant range.

An N/Q substitution at the Mg^{2+} block site of mammalian NR1 disrupts Mg^{2+} block and reduces Ca^{2+} permeability (Burnashev et al., 1992; Single et al., 2000), while a W/L substitution in the TM2 domain of NR2B disrupts Mg^{2+} block and increases Mg^{2+} permeability (Williams et al., 1998). This raises the possibility that Mg^{2+}-block-independent changes in channel kinetics and Mg^{2+} permeability may be responsible for the effects observed in our *dNR1*(*N631Q*)-expressing flies. While we cannot completely rule out this possibility, we observed increases in dCREB-2b protein in wild-type neurons in Mg^{2+}-free conditions, indicating that disruption of Mg^{2+} block, rather than changes in other channel properties, causes increased CREB repressor expression and decreased expression of LTM-associated genes.

A chronic elevation in extracellular Mg^{2+} enhances Mg^{2+} block of NMDARs, leading to upregulation of NMDAR activity and potentiation of NMDA-induced responses at positive membrane potentials (during correlated activity) (Slutsky et al., 2010). This raised the possibility that our Mg^{2+} block mutations may cause a downregulation of NMDAR-dependent signaling and decreased NMDA-induced responses at positive membrane potentials. Since we recorded NMDA-induced responses from various sizes of cells, we could not directly compare amplitudes of NMDA-induced responses between *elav/dNR1*(*wt*) cells and *elav/dNR1*(*N631Q*) cells. However, as seen in Figure S7, training-dependent

increases in ERK activity, required for CREB activation, occurred normally in both *elav/dNR1*(*wt*) cells and *elav/dNR1*(*N631Q*) cells, while it was significantly suppressed in *dNR1* hypomorphs. These results suggest that our Mg^{2+} block mutations do not alter NMDA-induced responses at positive membrane potentials.

Similar to *dNR1* Mg^{2+} block mutants, *dNR1* hypomorphic mutants also have defects in CREB-dependent gene expression upon LTM formation. However, *dNR1* hypomorphs and Mg^{2+} block mutants are likely to have opposing effects on Ca^{2+} influx. While hypomorphic *dNR1* mutants should have decreased Ca^{2+} influx during spaced training because of a reduction in the number of dNMDARs (Xia et al., 2005), *elav/dNR1*(*N631Q*) flies are unlikely to have this effect. Conversely, while *elav/dNR1*(*N631Q*) flies should have increased Ca^{2+} influx during the resting state when uncorrelated activity is likely to occur, *dNR1* hypomorphs should not. Supporting a model in which *dNR1* hypomorphs and Mg^{2+} block mutants inhibit LTM-dependent gene expression through different mechanisms, we show that Mg^{2+} block mutants increase basal expression of dCREB2-b repressor while NMDAR hypomorphs do not. Conversely, we also have data indicating that NMDAR hypomorphs are defective for training dependent increases in ERK activity, while *elav/dNR1*(*N631Q*) flies are not (Figure S7). These data fit a model in which there may be two equally important requirements for NMDARs in regulating LTM-dependent transcription (Figure 8B). First, during correlated, LTM-inducing stimulation, a large Ca^{2+} influx through channels, including NMDARs, may be required to activate kinases, including ERK, necessary to activate CREB. *dNR1* hypomorphs are defective for this process. However, a second and equally important requirement for NMDARs may be to inhibit low amounts of Ca^{2+} influx during uncorrelated activity to maintain the intracellular environment in a state conducive to CREB-dependent transcription. Mg^{2+} block is required for this process.

Although it is unclear what types of uncorrelated activity are suppressed by Mg^{2+} block, one type may be spontaneous, action potential (AP)-independent, single vesicle release events (referred to as “minis”). Supporting this idea, we observed an increase in dCREB2-b in cultured wild-type brains in Mg^{2+}-free medium in the presence of TTX (Figure 7E), which suppresses AP-dependent vesicle releases but does not affect minis. In addition, we observed a significant increase in cytosolic Ca^{2+}, $[Ca^{2+}]_i$, in response to 1 μM NMDA in the presence of extracellular Mg^{2+} in neurons from *elav/dNR1*(*N631Q*) pupae (Figure S8). In neurons from transgenic control and wild-type pupae, which have an intact Mg^{2+} block mechanism, 1 μM NMDA does not cause Ca^{2+} influx and membrane depolarization. The concentration of glutamate released by minis is on the order of 1 μM at the synaptic cleft (Hertz, 1979), suggesting that an increase in frequency of mini-induced Ca^{2+} influx due to decreased Mg^{2+} block may contribute to the increase in dCREB2-b in *elav/dNR1*(*N631Q*) flies.

Correlated, AP-mediated NMDAR activity has been proposed to facilitate dCREB2-dependent gene expression by increasing activity of a dCREB2 activator. Our present study suggests that, conversely, Mg^{2+} block functions to inhibit uncorrelated activity, including mini-dependent Ca^{2+} influx through NMDARs, which would otherwise cause increased dCREB2-b expression and decreased LTM (Figure 8B). Other studies have also suggested opposing roles of AP-mediated transmitter release and minis. For activity-dependent dendritic protein synthesis, local protein synthesis is stimulated by AP-mediated activity and inhibited by mini activity (Sutton et al., 2007). In the case of NMDARs, the opposing role of low Ca^{2+} influx in inhibiting CREB activity must be suppressed by Mg^{2+} block for proper LTM formation.

EXPERIMENTAL PROCEDURES

Fly Strains and Heat-Shock Regimen

Our wild-type control line *w*(*CS10*) has been described before (Tamura et al., 2003). All *Gal4* driver lines, *UAS-dNR1*(*wt*) and *UAS-dNR1*(*N631Q*) transgenic lines, *hs-dCREB2-b* (*17-2*) flies, and $dNR1^{EP3511}$ and $dNR1^{EP331}$ mutant flies were outcrossed to *w*(*CS10*) for at least six generations. Outcrossing of $homer^{R102}$ (gift from J.B. Thomas) was performed using RT-PCR analyses at each generation to identify flies carrying the mutation. Fly stocks were maintained at 25°C ± 2°C and 60% ± 10% relative humidity under a 12–12 hr, light-dark cycle.

The N631Q codon substitution in dNR1 was introduced by PCR mutagenesis using the QuikChange mutagenesis kit (Stratagene, La Jolla, CA, USA) using the following primers: 5′-TGGGGAGTCCTGCTGCAGAGCGGGATCGGCGAG-3′ and 5′-CTCGCCGATCCCGCTCTGCAGCAGGACTCCCCA-3′. To generate transgenic flies, the PCR product was subcloned into pUAST, a *Drosophila* expression vector, and injected with pUChspΔ2-3 containing helper transposase into *w*(*CS10*) embryos (Rubin and Spradling, 1982; Spradling and Rubin, 1982). We obtained three independent *UAS-dNR1*(*N631Q*) lines —*UAS-dNR1*(*N631Q*)-*M6*, *UAS-dNR1*(*N631Q*)-*M13*, and *UAS-dNR1* (*N631Q*)-*M15*—and two independent *UAS-dNR1*(*wt*) lines—*UAS-dNR1*(*wt*)-*W5* and *UAS-dNR1*(*wt*)-*W12*. In all experiments, *UAS-dNR1*(*N631Q*)-*M15* and *UAS-dNR1*(*wt*)-*W5* were used unless otherwise mentioned.

For heat-shock induction, flies were transferred to preheated vials and heat shocked at 35°C for the indicated amounts of time in a water bath. Heat shocks were given 3 hr prior to training and heat-shocked flies were returned to food vials during the recovery period. Before heat shock, flies were maintained in an 18°C incubator for at least 3 days to minimize leaky expression.

Cell Culture

Primary pupal CNS neurons were cultured as described (Su and O'Dowd, 2003). Heads were removed from pupae at pupal stage 8–10 (50–78 hr after pupation) in dissecting buffer containing (in mM) 126 NaCl, 5.4 KCl, 0.17 NaH_2PO_4, 0.22 KH_2PO_4, 33.3 glucose, 43.8 sucrose, and 9.9 HEPES (pH 7.4). Dissected brains, treated with (50 U/ml) papain and (1.32 mM) L-cysteine for 15 min at room temperature, were mechanically dissociated into suspensions of single cells in *Drosophila*-defined culture medium (DDM2) as described previously (Su and O'Dowd, 2003). Cells were placed on concanavalin-A–lamini-coated glass coverslips and cultured in a 23°C, humidified, 5% CO_2 incubator. Three- to four-day-old cultured neurons, which have not yet developed extensive connections, were used for electrophysiological and imaging analyses.

Electrophysiology

Whole-cell recordings, adapted from previous methods (Burnashev et al., 1992; Saitoe et al., 2001; Single et al., 2000; Xia et al., 2005), were performed on cultured neurons at room temperature. The internal solution in whole-cell pipettes (3–10 MΩ) contained (in mM) 158 KCl, 5 EGTA, 2 ATP, and 10 HEPES (pH 7.1). Hemolymph-like HL3 solution (Stewart et al., 1994) was used for the standard extracellular solution, and contained (in mM) 70 NaCl, 5 KCl, 10 $NaHCO_3$, 1.5 $CaCl_2$, 20 $MgCl_2$, 5 trehalose, 115 sucrose, and 5 HEPES (pH 7.2 with NaOH). High Na^+ extracellular solution contained (in mM) 140 NaCl, 1.5 $MgCl_2$, 5 KCl, 5 trehalose, 80 sucrose, and 5 HEPES (pH 7.2 with NaOH), while high Ca^{2+} extracellular solution contained 30 $CaCl_2$, 5 KCl, 70 N-methyl-D-glucamine, 5 trehalose, 115 sucrose, and 5 HEPES (pH 7.2 with $Ca(OH)_2$). The osmolarity of the solution was

adjusted with sucrose. In order to stabilize the surface potential, 1.5 mM $MgCl_2$ was added to the high Na^+ extracellular solution. dNMDARs do not demonstrate Mg^{2+} block at this concentration (Xia et al., 2005). For measuring Mg^{2+} permeability, Ca^{2+} and Na^+ in the HL3 solution were replaced to Mg^{2+} and N-methyl-D-glucamine, respectively, and the pH of the solution was adjusted using $Mg(OH)_2$. All chemicals dissolved in extracellular solution were delivered with a VC-6 valve controller (Warner Instruments, Novato, CA, USA). Data were acquired with an AXOPATCH-1D, a Digidata 1320A D-A converter, and pClamp 8 (Axon Instruments, Inverurie, Scotland) software.

P_{Ca}/P_{Na} was calculated using the Goldman-Hodgkin-Katz equation as described previously (Chang et al., 1994):

$$\begin{aligned} P_{\mathrm{Ca}}/P_{\mathrm{Na}} = \{([\mathrm{Na}^+]_i \\ -\alpha[\mathrm{Na}^+]_o)/(\alpha^2[\mathrm{Ca}^{2+}]_o \\ -[\mathrm{Ca}^{2+}]_i)\}(1+\alpha)/4 + (P_K/P_{\mathrm{Na}}) \times \{([K^+]_i \\ -\alpha[K^+]_o)/(\alpha^2[\mathrm{Ca}^{2+}]_o \\ -[\mathrm{Ca}^{2+}]_i)\}(1+\alpha)/4. \end{aligned} \quad (1)$$

$$\frac{P_K}{P_{\mathrm{Na}}} = \frac{([\mathrm{Na}^+]_i - \alpha[\mathrm{Na}^+]_o)}{(\alpha[K^+]_o - [K^+]_i)}, \quad (2)$$

where $\alpha = \exp(-FV_{rev}/RT)$ and V_{rev} is the reversal potential, and F, R, and T have their standard meanings.

Memory Assay

Single-Cycle Training—Standard single-cycle olfactory conditioning was performed as previously described (Tamura et al., 2003; Tully and Quinn, 1985). Two aversive odors (3-octanol [OCT] and 4-methylcyclohexanol [MCH]) were used as conditioned stimuli (CS). The unconditioned stimulus (US) was paired with one of the odors and consisted of 1.5 s pulses of 60 V DC electric shocks. To test for memory retention, about 100 trained flies were placed at the choice point of a T-maze in which they were exposed simultaneously to the CS+ (previously paired with the US) and CS- (unpaired with the US). As previously described (Tully et al., 1994), a performance index (PI) was calculated so that a 50:50 distribution (no memory) yielded a PI of zero and a 0:100 distribution away from the CS+ yielded a PI of 100. Peripheral control experiments, including odor acuity and shock reactivity assays, were performed as described previously (Tamura et al., 2003; Tully and Quinn, 1985) to verify that sensitivity to the odors and shock were unaffected in our transgenic flies.

Spaced and Massed Training—Repetitive spaced and massed trainings were performed as described previously (Tully et al., 1994; Xia et al., 2005). Spaced training consists of ten single-cycle trainings, where a 15 min rest interval is introduced between each session. Massed training consists of ten single-cycle trainings, where one session immediately follows the previous one. Memory was measured one day after spaced or massed training to evaluate LTM and ARM.

Short-Duration Training—Flies were exposed to CS+ and CS− odors for various durations (5, 10, 20, 30, and 60 s) and received electrical shocks every 5 s (1.5 s electric shock pulse) during exposure to the CS+. LRN was tested immediately after training. A training duration of 60 s corresponds to normal single cycle training.

Odor Specificity of Olfactory Learning—Flies were exposed to OCT for 60 s with (OCT+) or without (OCT−) electrical shocks (1.5 s pulses every 5 s). Immediately after training, flies were placed in a T-maze, where flies were exposed to an odor (OCT, MCH, or Benzaldehyde) and air simultaneously to examine whether training to OCT affects responses to unrelated odors.

Quantification of Transcripts

Transcript levels were quantified using real-time PCR (model 7500, Applied Biosystems, Carlsbad, CA, USA) as described previously (Yamazaki et al., 2007). Heads were harvested on dry ice, and total RNA was obtained using TRIzol reagent (Invitrogen, Carlsbad, CA, USA). cDNA was synthesized using a High-Capacity cDNA Archive Kit (Applied Biosystems), and qPCR was performed using sybr-green-based chemistry using specific primers (Table S1). Expression of each transcript was normalized to that of GAPDH1.

Immunoblotting and Immunohistochemistry

To generate anti-dNR1 antibody, rabbit antiserum (αNM1) was raised against the most C-terminal amino acid sequence of dNR1, CGKTRPQQSVLPPRYSP GYTSDVSHLVV. Affinity-purified antibody (1:1,000) was used for immunoblotting and immunohistochemistry as described previously (Xia et al., 2005). Fluorescence images of dNR1 distribution in fly brains were obtained using a confocal laser microscope (Fluoview FV500, Olympus, Shinjuku, Tokyo, Japan).

Immunoblotting protocols for dCREB2-b (Xia et al., 2005) and for ERK (MAPK) and pERK (pMAPK) (Pagani et al., 2009) have been previously described. Anti-dCREB2-b monoclonal antibody (Yin et al., 1994) was used at a 1:10 dilution. Anti-phospho-p44/42 MAPK and anti-total p44/42 MAPK primary antibodies were purchased from Cell Signaling Technology (Danvers, MA, USA) and used at a 1:1,000 dilution. Signals were detected using HRP conjugated secondary antibodies and ECL blotting reagents (GE Healthcare, Waukesha, WI, USA).

For analysis of dCREB2-b in single brains, adult heads were dissected and brains were placed in HL3 solution containing 100 μM TTX. After a first incubation in HL3 with TTX for 10 min in a 5% CO_2 incubator, the HL3 solution was replaced with Mg^{2+}-free HL3 solution ($SrCl_2$ was used instead of $MgCl_2$) and further incubated for 2 hr. To block dNMDAR activity in the Mg^{2+}-free condition, 1 mM MK801 was used when indicated. Single brains were homogenized in 10 μl lysis buffer and processed for immunoblotting as described previously.

Homer antibodies have been previously described (Diagana et al., 2002). For immunostaining, antibody was first preabsorbed overnight at 4°C with nitro-cellulose strips blotted with protein from *homer*^{R102} flies and then used at a dilution of 1:1,000 (Diagana et al., 2002). Immunostaining was performed as previously described (Diagana et al., 2002).

Statistical Analyses

All data are expressed as means ± SEM. Graph Pad Prism version 4.01 was used for statistical analyses. Statistical significance between two groups was analyzed by Student's t test. Significant differences between multiple groups were determined by one- or two-way ANOVA. Bonferroni/Dunn post hoc comparisons were used for individual comparisons after ANOVA.

Supplementary Material

Refer to Web version on PubMed Central for supplementary material.

Acknowledgments

We thank S. Ozawa, the late T. Tsujimoto, and the late Y. Kidokoro for comments on the preliminary draft of manuscript, as well as J. B. Thomas, A.-S. Chiang, T. Tamura, and S. Xia for fly stocks and U. Thomas for antibody. We also thank to A. Miwa and S. Hirai for assisting in experiments. We are grateful to members of the Saitoe laboratory for technical assistance and discussions. This work was supported by Takeda Science Foundation and the Uehara Memorial Foundation and by the Grant-in-Aid for Scientific Research on Innovative Areas "Systems Molecular Ethology" from the Ministry of Education, Culture, Sports, Science, and Technology (MEXT).

References

Adesnik H, Li G, During MJ, Pleasure SJ, Nicoll RA. NMDA receptors inhibit synapse unsilencing during brain development. Proc Natl Acad Sci USA. 2008; 105:5597–5602. [PubMed: 18375768]

Barco A, Alarcon JM, Kandel ER. Expression of constitutively active CREB protein facilitates the late phase of long-term potentiation by enhancing synaptic capture. Cell. 2002; 108:689–703. [PubMed: 11893339]

Begg M, Cruickshank WJ. A partial analysis of Drosophila larval haemolymph. Proc Roy SocEdingburgh. 1963; 68:215–236.

Bellinger FP, Wilce PA, Bedi KS, Wilson P. Long-lasting synaptic modification in the rat hippocampus resulting from NMDA receptor blockade during development. Synapse. 2002; 43:95–101. [PubMed: 11754487]

Bourtchuladze R, Frenguelli B, Blendy J, Cioffi D, Schutz G, Silva AJ. Deficient long-term memory in mice with a targeted mutation of the cAMP-responsive element-binding protein. Cell. 1994; 79:59–68. [PubMed: 7923378]

Brand AH, Perrimon N. Targeted gene expression as a means of altering cell fates and generating dominant phenotypes. Development. 1993; 118:401–415. [PubMed: 8223268]

Burnashev N, Schoepfer R, Monyer H, Ruppersberg JP, Günther W, Seeburg PH, Sakmann B. Control by asparagine residues of calcium permeability and magnesium blockade in the NMDA receptor. Science. 1992; 257:1415–1419. [PubMed: 1382314]

Chang H, Ciani S, Kidokoro Y. Ion permeation properties of the glutamate receptor channel in cultured embryonic Drosophila myotubes. J Physiol. 1994; 476:1–16. [PubMed: 7519261]

Cheng Y, Endo K, Wu K, Rodan AR, Heberlein U, Davis RL. Drosophila fasciclinII is required for the formation of odor memories and for normal sensitivity to alcohol. Cell. 2001; 105:757–768. [PubMed: 11440718]

Croghan PC, Lockwood APM. The composition of the haemolyph of the larva of Drosophila melanogaster. J Exp Biol. 1960; 37:339–343.

Diagana TT, Thomas U, Prokopenko SN, Xiao B, Worley PF, Thomas JB. Mutation of Drosophila homer disrupts control of locomotor activity and behavioral plasticity. J Neurosci. 2002; 22:428–436. [PubMed: 11784787]

Dubnau J, Chiang AS, Grady L, Barditch J, Gossweiler S, McNeil J, Smith P, Buldoc F, Scott R, Certa U, et al. The staufen/pumilio pathway is involved in Drosophila long-term memory. Curr Biol. 2003; 13:286–296. [PubMed: 12593794]

Ehrlich I, Malinow R. Postsynaptic density 95 controls AMPA receptor incorporation during long-term potentiation and experience-driven synaptic plasticity. J Neurosci. 2004; 24:916–927. [PubMed: 14749436]

Hertz L. Functional interactions between neurons and astrocytes I. Turnover and metabolism of putative amino acid transmitters. Prog Neurobiol. 1979; 13:277–323. [PubMed: 42117]

Hirasawa T, Wada H, Kohsaka S, Uchino S. Inhibition of NMDA receptors induces delayed neuronal maturation and sustained proliferation of progenitor cells during neocortical development. J Neurosci Res. 2003; 74:676–687. [PubMed: 14635219]

Inokuchi K, Kato A, Hiraia K, Hishinuma F, Inoue M, Ozawa F. Increase in activin beta A mRNA in rat hippocampus during long-term potentiation. FEBS Lett. 1996; 382:48–52. [PubMed: 8612762]

Kato A, Ozawa F, Saitoh Y, Hirai K, Inokuchi K. vesl, a gene encoding VASP/Ena family related protein, is upregulated during seizure, long-term potentiation and synaptogenesis. FEBS Lett. 1997; 412:183–189. [PubMed: 9257717]

Kato A, Fukazawa Y, Ozawa F, Inokuchi K, Sugiyama H. Activation of ERK cascade promotes accumulation of Vesl-1S/Homer-1a immunoreactivity at synapses. Brain Res Mol Brain Res. 2003; 118:33–44. [PubMed: 14559352]

Kuriu T, Inoue A, Bito H, Sobue K, Okabe S. Differential control of postsynaptic density scaffolds via actin-dependent and -independent mechanisms. J Neurosci. 2006; 26:7693–7706. [PubMed: 16855097]

Lüthi A, Schwyzer L, Mateos JM, Gähwiler BH, McKinney RA. NMDA receptor activation limits the number of synaptic connections during hippocampal development. Nat Neurosci. 2001; 4:1102–1107. [PubMed: 11687815]

Mao Z, Roman G, Zong L, Davis RL. Pharmacogenetic rescue in time and space of the rutabaga memory impairment by using Gene-Switch. Proc Natl Acad Sci USA. 2004; 101:198–203. [PubMed: 14684832]

Mayer ML, Westbrook GL, Guthrie PB. Voltage-dependent block by Mg2+ of NMDA responses in spinal cord neurones. Nature. 1984; 309:261–263. [PubMed: 6325946]

McKee JA, Brewer RP, Macy GE, Phillips-Bute B, Campbell KA, Borel CO, Reynolds JD, Warner DS. Analysis of the brain bioavailability of peripherally administered magnesium sulfate: a study in humans with acute brain injury undergoing prolonged induced hypermagnesemia. Crit Care Med. 2005; 33:661–666. [PubMed: 15753761]

Mizuno T, Kanazawa I, Sakurai M. Differential induction of LTP and LTD is not determined solely by instantaneous calcium concentration: an essential involvement of a temporal factor. Eur J Neurosci. 2001; 14:701–708. [PubMed: 11556894]

Mori H, Masaki H, Yamakura T, Mishina M. Identification by mutagenesis of a Mg(2+)-block site of the NMDA receptor channel. Nature. 1992; 358:673–675. [PubMed: 1386653]

Nowak L, Bregestovski P, Ascher P, Herbet A, Prochiantz A. Magnesium gates glutamate-activated channels in mouse central neurones. Nature. 1984; 307:462–465. [PubMed: 6320006]

Osterwalder T, Yoon KS, White BH, Keshishian H. A conditional tissue-specific transgene expression system using inducible GAL4. Proc Natl Acad Sci USA. 2001; 98:12596–12601. [PubMed: 11675495]

Pagani MR, Oishi K, Gelb BD, Zhong Y. The phosphatase SHP2 regulates the spacing effect for long-term memory induction. Cell. 2009; 139:186–198. [PubMed: 19804763]

Rosenblum K, Futter M, Voss K, Erent M, Skehel PA, French P, Obosi L, Jones MW, Bliss TV. The role of extracellular regulated kinases I/II in late-phase long-term potentiation. J Neurosci. 2002; 22:5432–5441. [PubMed: 12097495]

Rubin GM, Spradling AC. Genetic transformation of Drosophila with transposable element vectors. Science. 1982; 218:348–353. [PubMed: 6289436]

Saitoe M, Schwarz TL, Umbach JA, Gundersen CB, Kidokoro Y. Absence of junctional glutamate receptor clusters in Drosophila mutants lacking spontaneous transmitter release. Science. 2001; 293:514–517. [PubMed: 11463917]

Silva AJ, Kogan JH, Frankland PW, Kida S. CREB and memory. Annu Rev Neurosci. 1998; 21:127–148. [PubMed: 9530494]

Single FN, Rozov A, Burnashev N, Zimmermann F, Hanley DF, Forrest D, Curran T, Jensen V, Hvalby O, Sprengel R, Seeburg PH. Dysfunctions in mice by NMDA receptor point mutations NR1(N598Q) and NR1(N598R). J Neurosci. 2000; 20:2558–2566. [PubMed: 10729336]

Skeberdis VA, Chevaleyre V, Lau CG, Goldberg JH, Pettit DL, Suadicani SO, Lin Y, Bennett MV, Yuste R, Castillo PE, Zukin RS. Protein kinase A regulates calcium permeability of NMDA receptors. Nat Neurosci. 2006; 9:501–510. [PubMed: 16531999]

Skoulakis EM, Davis RL. Olfactory learning deficits in mutants for leonardo, a Drosophila gene encoding a 14-3-3 protein. Neuron. 1996; 17:931–944. [PubMed: 8938125]

Slutsky I, Sadeghpour S, Li B, Liu G. Enhancement of synaptic plasticity through chronically reduced Ca2+ flux during uncorrelated activity. Neuron. 2004; 44:835–849. [PubMed: 15572114]

Slutsky I, Abumaria N, Wu LJ, Huang C, Zhang L, Li B, Zhao X, Govindarajan A, Zhao MG, Zhuo M, et al. Enhancement of learning and memory by elevating brain magnesium. Neuron. 2010; 65:165–177. [PubMed: 20152124]

Spradling AC, Rubin GM. Transposition of cloned P elements into Drosophila germ line chromosomes. Science. 1982; 218:341–347. [PubMed: 6289435]

Stewart BA, Atwood HL, Renger JJ, Wang J, Wu CF. Improved stability of Drosophila larval neuromuscular preparations in haemolymph-like physiological solutions. J Comp Physiol A Neuroethol Sens Neural Behav Physiol. 1994; 175:179–191.

Su H, O'Dowd DK. Fast synaptic currents in Drosophila mushroom body Kenyon cells are mediated by alpha-bungarotoxin-sensitive nicotinic acetylcholine receptors and picrotoxin-sensitive GABA receptors. J Neurosci. 2003; 23:9246–9253. [PubMed: 14534259]

Sutton MA, Taylor AM, Ito HT, Pham A, Schuman EM. Postsynaptic decoding of neural activity: eEF2 as a biochemical sensor coupling miniature synaptic transmission to local protein synthesis. Neuron. 2007; 55:648–661. [PubMed: 17698016]

Tamura T, Chiang AS, Ito N, Liu HP, Horiuchi J, Tully T, Saitoe M. Aging specifically impairs amnesiac-dependent memory in Drosophila. Neuron. 2003; 40:1003–1011. [PubMed: 14659098]

Tanimoto K, Yoshida E, Mita S, Nibu Y, Murakami K, Fukamizu A. Human activin betaA gene. Identification of novel 5′ exon, functional promoter, and enhancers. J Biol Chem. 1996; 271:32760–32769. [PubMed: 8955111]

Tian L, Stefanidakis M, Ning L, Van Lint P, Nyman-Huttunen H, Libert C, Itohara S, Mishina M, Rauvala H, Gahmberg CG. Activation of NMDA receptors promotes dendritic spine development through MMP-mediated ICAM-5 cleavage. J Cell Biol. 2007; 178:687–700. [PubMed: 17682049]

Tully T, Quinn WG. Classical conditioning and retention in normal and mutant Drosophila melanogaster. J Comp Physiol A Neuroethol Sens Neural Behav Physiol. 1985; 157:263–277.

Tully T, Preat T, Boynton SC, Del Vecchio M. Genetic dissection of consolidated memory in Drosophila. Cell. 1994; 79:35–47. [PubMed: 7923375]

Williams K, Pahk AJ, Kashiwagi K, Masuko T, Nguyen ND, Igarashi K. The selectivity filter of the N-methyl-D-aspartate receptor: a tryptophan residue controls block and permeation of Mg2+ Mol Pharmacol. 1998; 53:933–941. [PubMed: 9584221]

Wu CL, Xia S, Fu TF, Wang H, Chen YH, Leong D, Chiang AS, Tully T. Specific requirement of NMDA receptors for long-term memory consolidation in Drosophila ellipsoid body. Nat Neurosci. 2007; 10:1578–1586. [PubMed: 17982450]

Xia S, Miyashita T, Fu TF, Lin WY, Wu CL, Pyzocha L, Lin IR, Saitoe M, Tully T, Chiang AS. NMDA receptors mediate olfactory learning and memory in Drosophila. Curr Biol. 2005; 15:603–615. [PubMed: 15823532]

Yamazaki D, Horiuchi J, Nakagami Y, Nagano S, Tamura T, Saitoe M. The Drosophila DCO mutation suppresses age-related memory impairment without affecting lifespan. Nat Neurosci. 2007; 10:478–484. [PubMed: 17322874]

Yin JC, Tully T. CREB and the formation of long-term memory. Curr Opin Neurobiol. 1996; 6:264–268. [PubMed: 8725970]

Yin JC, Wallach JS, Del Vecchio M, Wilder EL, Zhou H, Quinn WG, Tully T. Induction of a dominant negative CREB transgene specifically blocks long-term memory in Drosophila. Cell. 1994; 79:49–58. [PubMed: 7923376]

Zachepilo TG, Il'inykh YF, Lopatina NG, Molotkov DA, Popov AV, Savvateeva-Popova EV, Vaido AI, Chesnokova EG. Comparative analysis of the locations of the NR1 and NR2 NMDA receptor subunits in honeybee (Apis mellifera) and fruit fly (Drosophila melanogaster, Canton-S wild-type) cerebral ganglia. Neurosci Behav Physiol. 2008; 38:369–372. [PubMed: 18401728]

Zannat MT, Locatelli F, Rybak J, Menzel R, Leboulle G. Identification and localisation of the NR1 sub-unit homologue of the NMDA glutamate receptor in the honeybee brain. Neurosci Lett. 2006; 398:274–279. [PubMed: 16480817]

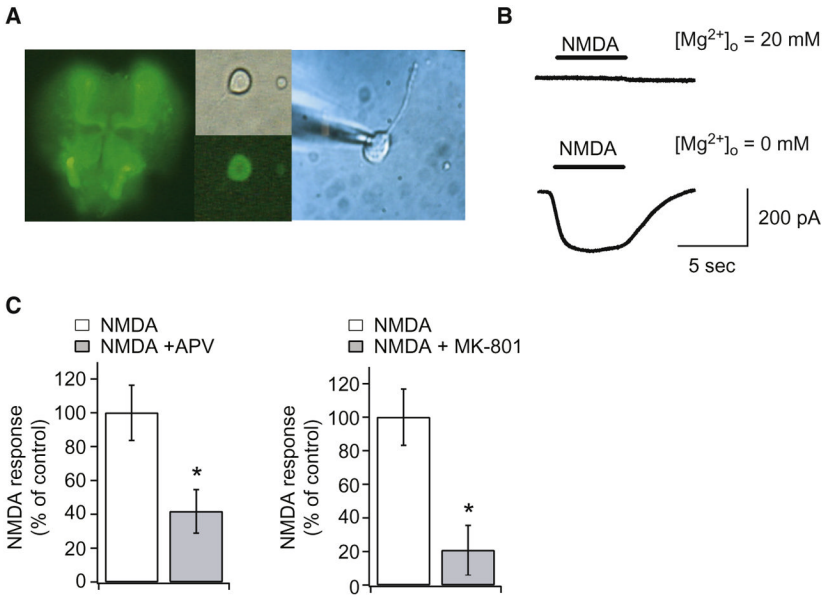

Figure 1. Physiological and Pharmacological Properties of Endogenous dNMDARs in the Fly Brain

(A) The pupal neuronal primary culture system. (Left) GFP image of neurons in an intact *elav/GFP* pupal brain. (Middle) A phase contrast image of a neuron dissociated from the pupal brain (upper) and its GFP signal (lower). (Right) Whole-cell clamping of a GFP-positive neuron. See also Figure S1 for dNR1 distribution.

(B) Inward currents induced by 100 μM NMDA in GFP-positive cells are abolished in the presence of 20 mM Mg^{2+}. GFP-positive cells responded to NMDA at 0 mM Mg^{2+}.

(C) Both NMDAR antagonists APV (10 μM) and MK-801 (10 μM) significantly decrease NMDA-activated currents in GFP-positive neurons. *$p < 0.05$ by t test. $n = 6$ for all data. Error bars in all figures in this paper indicate SEM.

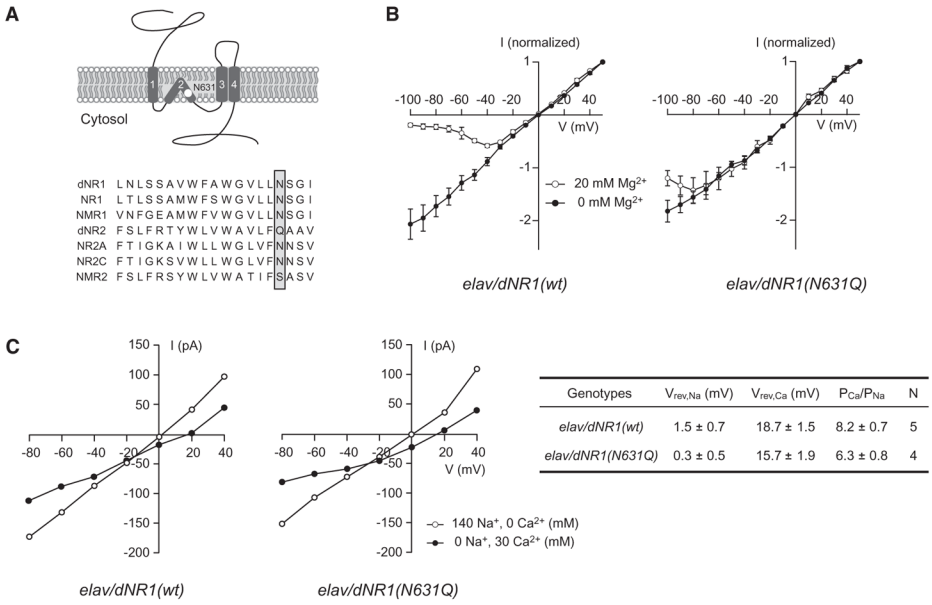

Genotypes	$V_{rev,Na}$ (mV)	$V_{rev,Ca}$ (mV)	P_{Ca}/P_{Na}	N
elav/dNR1(wt)	1.5 ± 0.7	18.7 ± 1.5	8.2 ± 0.7	5
elav/dNR1(N631Q)	0.3 ± 0.5	15.7 ± 1.9	6.3 ± 0.8	4

Figure 2. Suppression of dNMDAR Mg^{2+} Block in Neurons from Transgenic Pupae Overexpressing dNR1(N631Q)

(A) Schematic diagram of dNR1 and amino acid sequence comparisons of the TM2 domains of *Drosophila* (dNR1 and dNR2), mouse (NR1, NR2A, and NR2C), and *C. elegans* (NMR1 and NMR2) NMDAR subunits. The white circle (upper) and shadowed box (lower) indicate the Mg^{2+} block site in the TM2 domain.

(B) Current-voltage (I-V) curves generated from neurons from *elav/dNR1*(*wt*) (n = 6) and *elav/dNR1*(*N631Q*) pupae (n = 6). Currents elicited by 100 μM NMDA were normalized to peak responses at +50 mV. Due to Mg^{2+} block, all examined neurons from *elav/dNR1*(*wt*) displayed a typical J-shaped I-V relation in the presence of 20 mM extracelluar Mg^{2+}.

(C) (Left) I-V relationships in high Na^+ (open circle) and high Ca^{2+} (closed circle) extracellular solutions for *elav/dNR1*(*wt*) and *elav/dNR1*(*N631Q*) neurons. I-V relationships in each extracellular solution were recorded from the same neuron after confirming the presence [for *elav/dNR1*(*wt*)] or absence [for *elav/dNR1*(*N631Q*)] of Mg^{2+} block. (Right) Reversal potentials in high Na^+ extracellular solution ($V_{rev,Na}$) and in high Ca^{2+} extracellular solution ($V_{rev,Ca}$) were measured from the left panel, and relative Ca^{2+} permeabilities (P_{Ca}/P_{Na}) were calculated using the Goldman-Hodgkin-Katz (GHK) equation.

See also Figures S2 and S3.

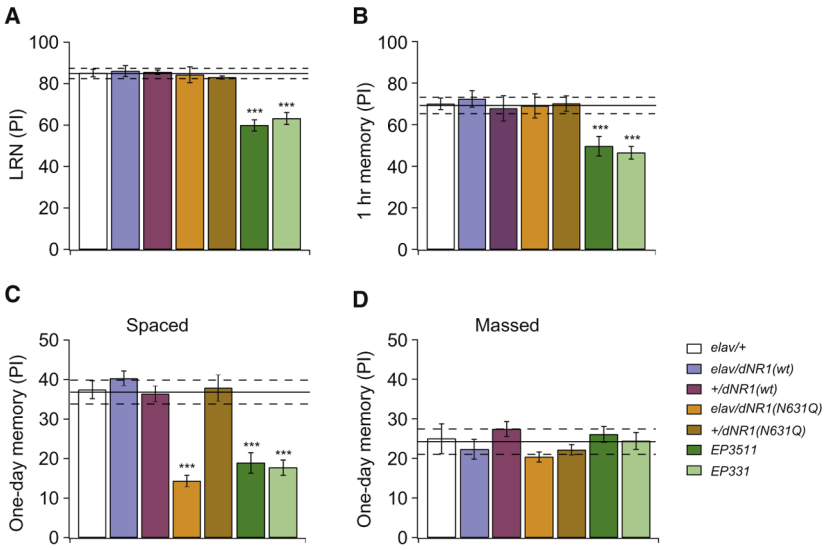

Figure 3. Transgenic *elav/dNR1*(*N631Q*) Flies Are Defective for Long-Term Memory but Not Learning

(A) In contrast to $dNR1^{EP3511}$ (*EP3511*) and $dNR1^{EP331}$ (*EP331*) hypomorphs, learning (LRN) is normal in *elav/dNR1*(*wt*) and *elav/dNR1*(*N631Q*) flies.

(B) Short-term memory is normal in *elav/dNR1*(*wt*) and *elav/dNR1*(*N631Q*) flies and reduced in $dNR1^{EP3511}$ (*EP3511*) and $dNR1^{EP331}$ (*EP331*) hypomorphs.

(C) One-day memory after spaced training is reduced in *elav/dNR1*(*N631Q*) flies and in *dNR1* hypomorphs.

(D) One-day memory after massed training is normal in *elav/dNR1*(*N631Q*) flies and in *dNR1* hypomorphs.

In all panels, data from wild-type flies are indicated by the solid (mean) and dotted (SEM) lines. ***$p < 0.0001$, as determined by one-way ANOVA and Bonferroni post hoc analyses. n = 8 to 10 for all data.

See also Figures S3 and S5.

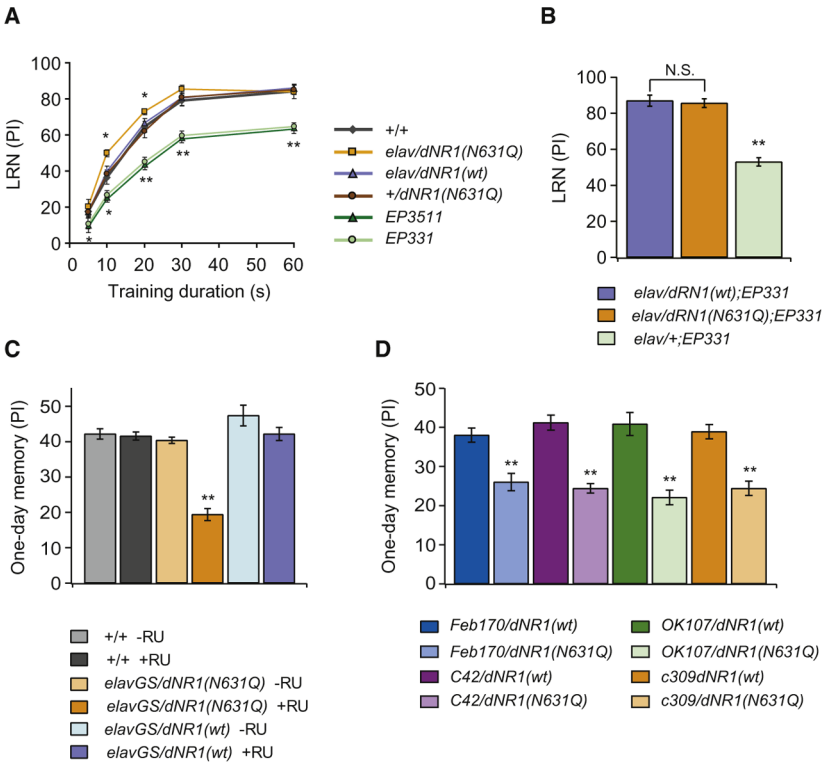

Figure 4. Mg^{2+} Block Is Physiologically Required for LTM Formation

(A) LRN assayed using a short-duration training paradigm. LRN PI scores increase progressively as a function of training duration. Mg^{2+} block mutations do not inhibit LRN. Rather, *elav/dNR1*(*N631Q*) flies have slightly improved LRN compared to other transgenic control flies at training durations of 10 and 20 s. *p < 0.05 and **p < 0.01, n = 8–12 for all data.

(B) Expression of a *dNR1*(*N631Q*) transgene restores normal memory in $dNR1^{EP331}$ mutants. **p < 0.01, n = 6–8 for all data.

(C) Acute feeding of 1 mM RU486, starting one day prior to training, significantly impairs LTM formation in *elavGS/dNR1*(*N631Q*) flies. **p < 0.001, n = 8–12 for all data.

(D) Expression of a *dNR1*(*N631Q*) transgene in the ellipsoid body of the central complex, *Feb170/dNR1*(*N631Q*) and *C42/dNR1*(*N631Q*), and in the MBs, *OK107/dNR1*(*N631Q*) and *C309/dNR1*(*N631Q*), significantly impairs LTM formation. **p < 0.001, n = 10 for all data. See also Figure S4.

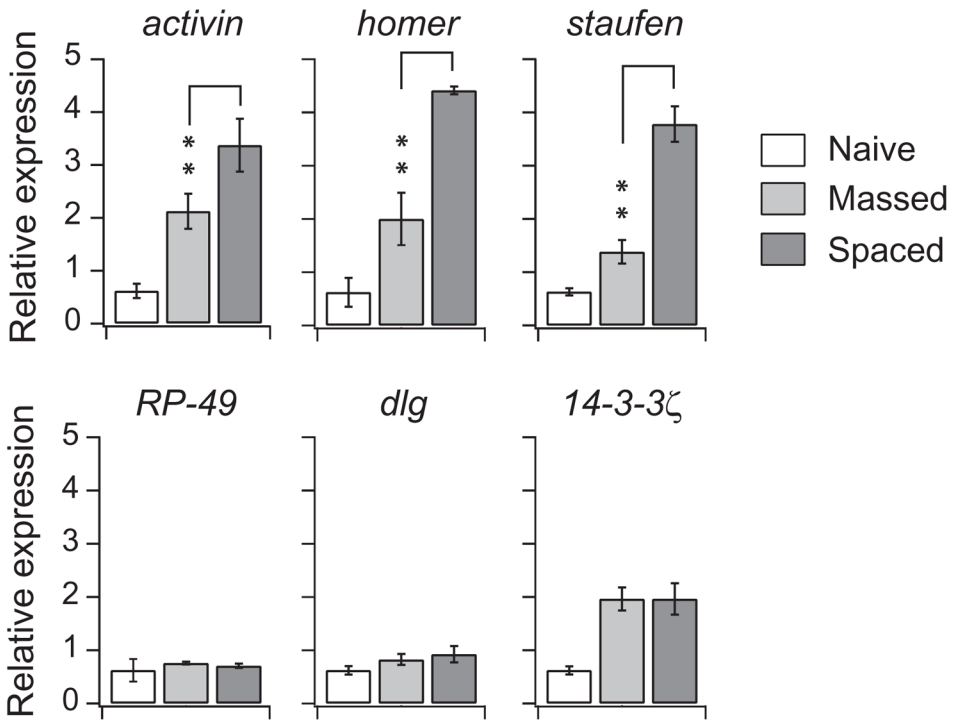

Figure 5. LTM-Dependent Induction of *activin*, *homer*, and *staufen* Expression

Increased transcription of *activin*, *staufen*, and *homer* is observed 6 hr after spaced training. Expression is significantly higher after spaced training than after massed training. Expression of *RP-49* (ribosomal protein), *dlg*, and *14-3-3ζ* are the same after spaced and massed training. Expression of all genes was normalized to expression of GAPDH1. Comparison of gene expression 3 and 24 hr after spaced versus massed training gave similar results (data not shown). One-way ANOVA indicates significant differences due to training protocol for *activin*, *homer*, and *staufen*. **$p < 0.001$ as determined by Bonferroni post hoc analyses, $n = 10$ for all data.

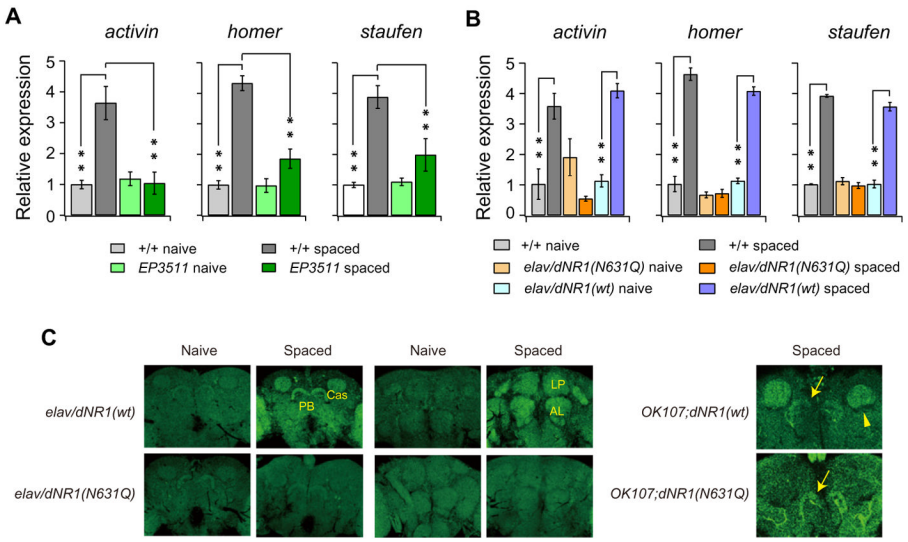

Figure 6. NMDARs and Mg^{2+} Block Are Required for LTM-Dependent Increases in *activin*, *homer*, and *staufen* Expression

(A) The increase in transcription of *activin*, *homer*, and *staufen* 6 hr after spaced training is suppressed in hypomorphic $dNR1^{EP3511}$ (*EP3511*) flies. Two-way ANOVA indicates significant differences due to training, genotype, and interaction between training and genotype. **p < 0.001 determined by Bonferroni post hoc comparisons. n = 10 for all data.

(B) The increase in transcription of *activin*, *homer*, and *staufen* after spaced training in wild-type and transgenic control *elav/dNR1*(*wt*) flies is abolished in *elav/dNR1*(*N631Q*) Mg^{2+} block mutant flies. Two-way ANOVA indicates significant differences due to training, genotype, and interaction between training and genotype. **p < 0.001. n = 10 for all data.

(C) Spaced training causes increases in HOMER protein in various brain regions, including the calyces of the MBs (Cas), protocerebral bridge (PB), the antennal lobes (ALs), and lateral protocerbrum (LP). These increases do not occur in brains of *elav/dNR1*(*N631Q*) flies. Restricting *dNR1*(*N631Q*) expression to the MBs prevents increases in HOMER protein in the Cas (yellow arrowhead) but does not affect expression in the PB (yellow arrows).

See also Figure S6.

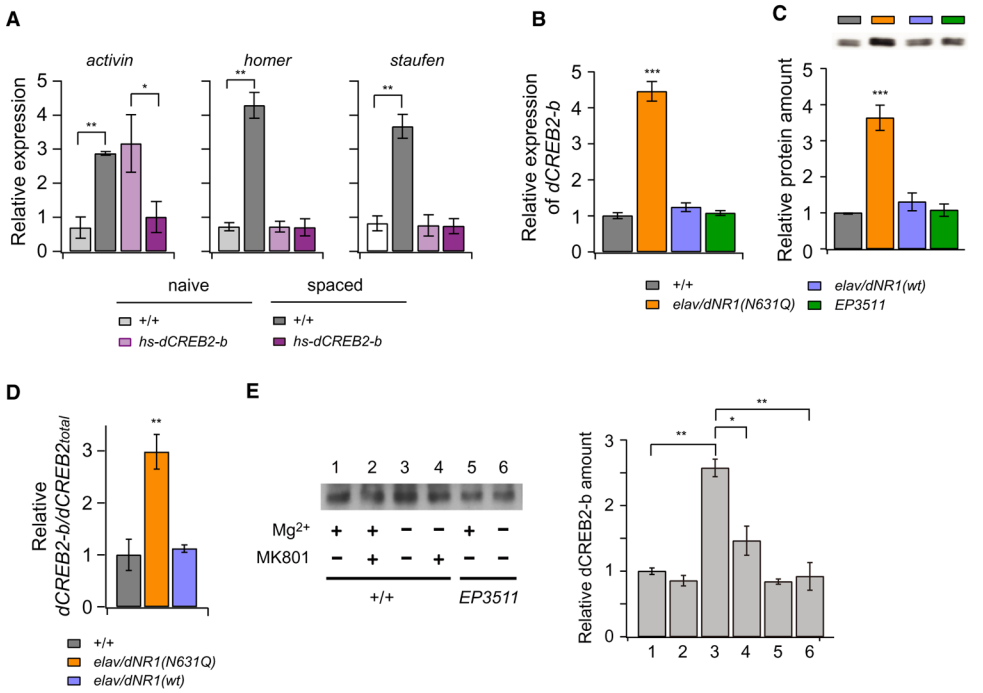

Figure 7. Mg^{2+} Block Is Required for CREB-Dependent Induction of LTM-Associated Genes

(A) The increase in *activin*, *homer*, and *staufen* transcription after spaced training does not occur in heat-shocked *hs-dCREB2-b* (*17-2*) flies. Two-way ANOVA indicates significant differences due to genotype, training, and interaction between genotype and training. **p < 0.01 and *p < 0.03, determined by Bonferroni post hoc comparisons, n = 8–12 for all data.

(B) Basal expression of *dCREB2-b* transcripts is significantly increased in *elav/dNR1*(*N631Q*) flies. One-way ANOVA indicates significant differences due to genotype. ***p < 0.001 compared to +/+ and *elav/dNR1*(*wt*) flies, n = 10 for all data. The wild-type level of *dCREB2-b* expression (normalized to GAPDH1 expression) was defined as 1.

(C) dCREB2-b protein is significantly increased in *elav/dNR1*(*N631Q*) flies but not in $dNR1^{EP3511}$ flies. dCREB2-b protein was normalized using tubulin, and the wild-type amount was defined as 1. One-way ANOVA indicates significant differences due to genotype. ***p < 0.001 compared to +/+ and *elav/dNR1*(*wt*) flies, n = 10 for all data.

(D) Comparison of $dCREB2\text{-}b/dCREB_{total}$ ratios. The ratio of repressor to total dCREB2 ($dCREB2\text{-}b/dCREB_{total}$) is increased more than 2-fold in *elav/dNR1(N631Q)* flies compared to wild-type and *elav/dNR1*(*wt*) flies. One-way ANOVA indicates significant differences due to genotype. **p < 0.01, n = 10 for all data.

(E) Removal of external Mg^{2+} increases dCREB2-b protein in cultured brains. A greater than 2-fold increase in dCREB2-b protein was observed in single brains dissected from adult flies, cultured in the absence of external Mg^{2+}. This increase was suppressed by the NMDAR antagonist MK801 and by the $dNR1^{EP3511}$ mutation. TTX was added to all cultures to suppress action potentials. One-way ANOVA indicates significant differences due to genotype. **p < 0.01 and *p < 0.05, n = 6 for all data.

See also Figure S7.

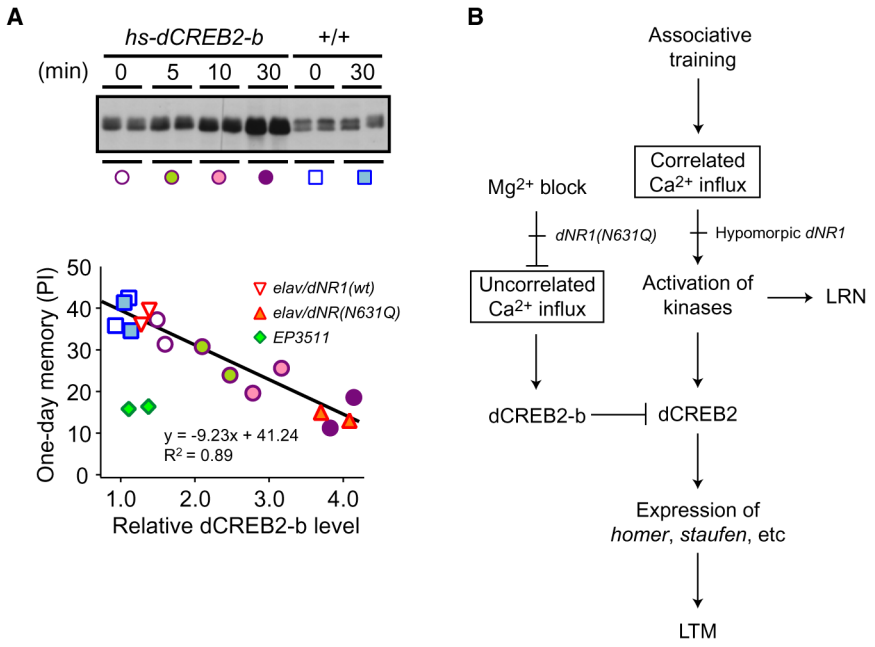

Figure 8. Mg^{2+} Block of dNMDARs Functions to Suppress dCREB2-b Expression

(A) Correlation between amounts of dCREB2-b protein and defects in LTM. Wild-type (+/+) and *hs-dCREB2-b* flies were heat shocked at 35°C for various durations (min) and separated into two groups. One group was used for immunoblotting to quantify the amounts of dCREB2-b protein (upper panel), and the second group was subjected to spaced-training. (Lower panel) LTM scores (one-day memory after spaced training) are plotted against the amounts of dCREB2-b protein in flies heat shocked for the indicated times. The dCREB2-b/tubulin ratio was normalized to that of wild-type without heat shock. As seen from the regression line obtained from wild-type and *hs-dCREB2-b* flies, the amount of dCREB2-b in *elav/dNR1(N631Q)* flies is sufficient to disrupt LTM formation.

(B) A model for Mg^{2+} block function in LTM formation. Ca^{2+} influx during correlated activity activates adenylyl cyclase and kinases, including CaMKs, ERK, and PKA, promoting associative learning and dCREB2-dependent induction of LTM-associated genes. Ca^{2+} influx during uncor-related activity, driven by unpaired stimuli and by “minis,” is usually prevented by Mg^{2+} block. In the absence of Mg^{2+} block, low Ca^{2+} influx from unpaired stimuli and minis increases a repressor isoform dCREB2-b, preventing formation of LTM. See also Figure S7.